PAPER

Low-voltage and high-performance buzzer-scanner based streamlined atomic force microscope system

To cite this article: Wei-Min Wang *et al* 2013 *Nanotechnology* **24** 455503

Nanotechnology **24** (2013) 455503 (8pp) doi:10.1088/0957-4484/24/45/455503

Low-voltage and high-performance buzzer-scanner based streamlined atomic force microscope system

Wei-Min Wang[1,2], Kuang-Yuh Huang[2], Hsuan-Fu Huang[1,2], Ing-Shouh Hwang[1] and En-Te Hwu[1]

[1] Institute of Physics, Academia Sinica, Taipei, 11529, Taiwan
[2] Department of Mechanical Engineering, National Taiwan University, Taipei, 10617, Taiwan

E-mail: whoand@gmail.com

Received 23 May 2013, in final form 19 September 2013
Published 18 October 2013
Online at stacks.iop.org/Nano/24/455503

Abstract

In this paper we present a novel scanner design in a quad-rod actuation structure, actuated by piezoelectric disk buzzers, and a new type of atomic force microscope (AFM), which uses this buzzer-scanner and a compact disk/digital-versatile-disk astigmatic optical pickup unit (OPU) for the detection of cantilever movements. Commercially available piezoelectric disk buzzers have a low capacitance and can be driven by low-voltage signal sources, such as analog outputs from a data acquisition card, without additional voltage or current amplifiers. Various scanning ranges can be realized through changing the dimensions of the actuation structure and/or the choice of disk buzzer. We constructed a buzzer-scanner and evaluated its performance. The scanner had a scanning range of 15 μm in the X and Y directions and an actuation range of 3.5 μm on the Z axis, with nonlinearity of 2.11%, 2.73%, and 2.19% for the X, Y and Z axes, respectively. The scanner had a resonance frequency of approximately 360 Hz on the X and Y axes, and 4.12 kHz on the Z axis. An OPU-AFM with this buzzer-scanner can resolve single atomic steps of a graphite substrate with a noise level of 0.06 nm. The obtained topographic images exhibit much less distortion than those obtained with an AFM using a piezoelectric tube scanner.

(Some figures may appear in colour only in the online journal)

1. Introduction

Scanning probe microscopy (SPM) [1] and atomic force microscopy (AFM) [2] have been applied to a wide variety of fields for nanometer-scale imaging and measurement. Applications range from physical, engineering and life sciences, to process development and control. Through long-term progressive improvement, AFMs have become an accessible and easy-to-use nanotechnology tool for studying the physical properties of material surfaces [3]. It is thus highly desirable to reduce the cost of this precision instrument, so that the AFM can become a common laboratory tool, as is the optical microscope. However, current commercial AFMs are expensive because of the high cost of their construction. One major expense arises from the complicated optical detection module used for measuring the nanometer-scale deflections of a microfabricated cantilever. An optical module using the beam-deflection detection method can cost over US$5000. In recent years, it has been demonstrated that compact disk/digital-versatile-disk (CD/DVD) optical pickup units (OPUs) can measure the sub-atomic displacements of an AFM probe [4–6]. Current OPUs typically adopt an astigmatic optical path—the detection spot size can be smaller than 1 μm, and the measuring bandwidth can reach over 60 MHz. The commercial OPU weighs approximately 18 g or less and costs less than US$20. A commercial AFM modified with an OPU for detection of cantilever resonance shows an image quality equivalent to that obtained with the commercial beam-deflection module [5, 6]. In addition, an anti-drift mechanism has been successfully

applied in an OPU-AFM system for focusing the laser beam on the cantilever, and for drift compensation [7]. This OPU-AFM also has an optical profiler mode that uses the focused laser beam to scan the surface without any tip and obtain the surface profile at high speed [8].

Another expense arises from the scanner, as well as from the electronics that drive the scanner for precision positioning of the sample relative to the probe and for the high-resolution scanning motion. Several types of scanners are currently used in AFMs. A piezoelectric tube scanner [9] is most commonly adopted in AFMs because of its simple and compact design. The tube scanner is made of a thin and brittle ceramic material, and can easily be broken by heavy loads, mechanical impact, or high-voltage pulses. A tube scanner costs over US$1000. This kind of scanner needs to be driven by expensive low-noise, high-voltage (±200 V) amplifiers. In addition, a bow-shaped distortion often appears in large-scan images of flat surfaces taken with the tube scanners, because of coupling of the XY movements with the Z movement. Thus, post-image processing is required for removal of the distortion. Another type of scanner, with a mechanical flexural guiding design [10, 11], can provide mechanical amplifiers for a larger scanning range, and linear guides for high-quality linear movements. The flexural scanners are usually driven by piezoelectric stacks and provide scanning with crosstalk less than 0.1%. However, the flexural scanner requires precision fabrication and assembly for its piezoelectric stacks and low-noise high-voltage driving electronics, all of which are expensive. In addition, nonlinear characteristics of the piezoelectric elements, such as the creep [12, 13] and the hysteresis [14, 15] effects, are amplified by the structure. Frequent calibrations or installation of feedback sensors are required for high-quality measurements of the AFM systems.

The piezoelectric buzzer uses transducers that convert electrical signals to sound waves, and is applied in watches and numerous other consumer electronics devices. The disk buzzer is a monomorph type that is composed of a thin piezoelectric layer and a brass diaphragm, as shown in figure 1(a). The brass diaphragm is grounded and the piezoelectric layer expands or contracts in response to the applied voltage, deforming the disk buzzer in concave upward or downward deformation depending on the voltage polarity, as shown in figures 1(b) and (c). In 1999, Alexander *et al* reported a scanner based on a single, commercial piezoelectric disk buzzer [16]. In that scanner design, the electrode of the piezoelectric layer on the buzzer was cut into four quadrants. A sample or an AFM probe was placed on one end of a rod, the other end of which was glued to the center of the buzzer. The three-dimensional (3D) movements of the scanner were achieved by actuating specific quadrants of the piezoelectric layer. The advantages of using the disk buzzer-scanner include compactness, economic benefits, and simple design. Additionally, the disk scanner can be driven by low-voltage signals of −10 to +10 V. However, the scanning range of this scanner design is small, which limits its application to scanning tunneling microscopy (STM). Even though a longer rod may enlarge the XY scanning range, the scanner rigidity degrades dramatically.

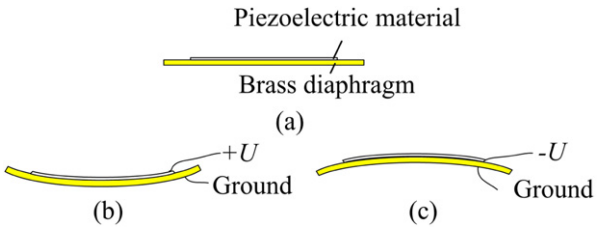

Figure 1. Working principle of a piezoelectric disk buzzer. (a) Monomorph buildup. (b) The brass diaphragm is grounded. A positive voltage applied to the piezoelectric layer causes a concave upward deformation of the disk buzzer. (c) A negative voltage induces a concave downward deformation.

In this paper, we demonstrate a new design for a low-voltage piezoelectric buzzer-scanner with a sufficient scanning area. A quad-rod actuation structure containing multiple piezoelectric disk buzzers results in favorable system stiffness. Characteristics of this buzzer-scanner, such as nonlinearity, resonance frequencies, and orthogonality, are evaluated and compared with those of a tube scanner. We constructed an economically streamlined AFM that uses this type of buzzer-scanner and an OPU for measuring the cantilever resonance. In terms of spatial resolution, image quality, and scanning speed, this AFM has a performance equivalent to most current commercial AFMs.

2. Buzzer-scanner

The buzzer-scanner consists of five piezoelectric disk buzzers, as shown in figure 2(a). Two pairs of buzzers $(X, -X)$ and $(Y, -Y)$ are fixed on two sides of the scanner base plate in perpendicular directions, and the final buzzer is fixed on top of the scanner upper plate for the Z-axis actuation. The base plate and the upper plate are both made of aluminum. A sample holder is attached through a magnet glued to the center of the Z-axis buzzer. A quad-rod actuation structure is composed of four carbon-fiber rods glued to the scanner's upper plate on one end and to the center of each of the four disk buzzers on the other end. Figure 2(b) shows the deformation of one pair of buzzers $(X, -X)$ when voltages of opposite polarities are applied, resulting in the lateral displacement $\pm\Delta l_x$ of the sample holder along the X axis. The vertical linear deformations $\pm\Delta l_z$ of the two disk buzzers lead to an angular tilt θ_y of the scanner. As a result, the sample holder is displaced laterally approximately in the X direction from its original position. The same working principle is applied for displacement in the Y direction. The buzzer on the Z holder moves the sample holder upward or downward during actuation, as illustrated in figures 1(b) and (c).

Figure 2(b) shows related parameters of the actuation structure, and the displacement on the two disk buzzers when voltages of opposite polarities are applied. The vertical deformation of the buzzer Δl_z can lead to an angular tilt θ_y of the scanner, which provides a lateral displacement Δl_x of the sample holder. We can derive the following relationship:

$$\Delta l_x = (l + l_{\mathrm{m}}) \sin\theta_y \cong \frac{l + l_{\mathrm{m}}}{r} \cdot \Delta l_z, \qquad (1)$$

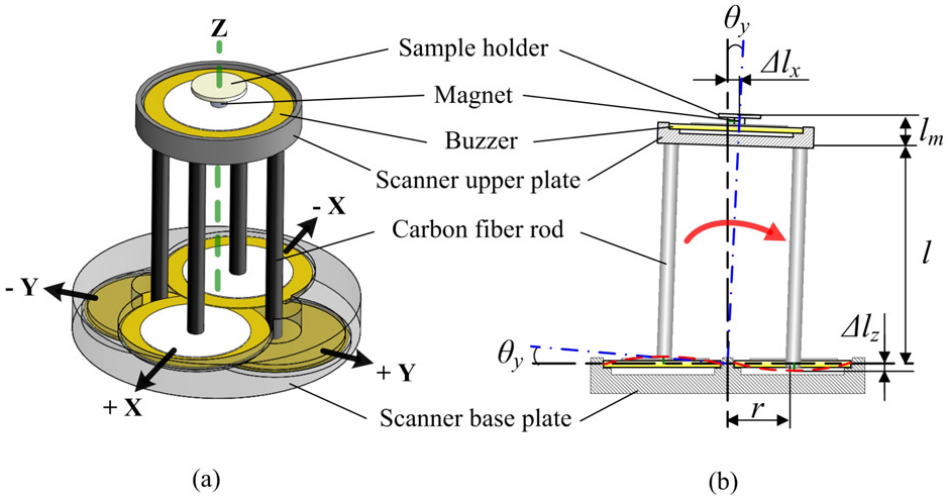

Figure 2. (a) Schematic configuration of the buzzer-scanner. (b) Dimensional and motional parameters of the buzzer-scanner.

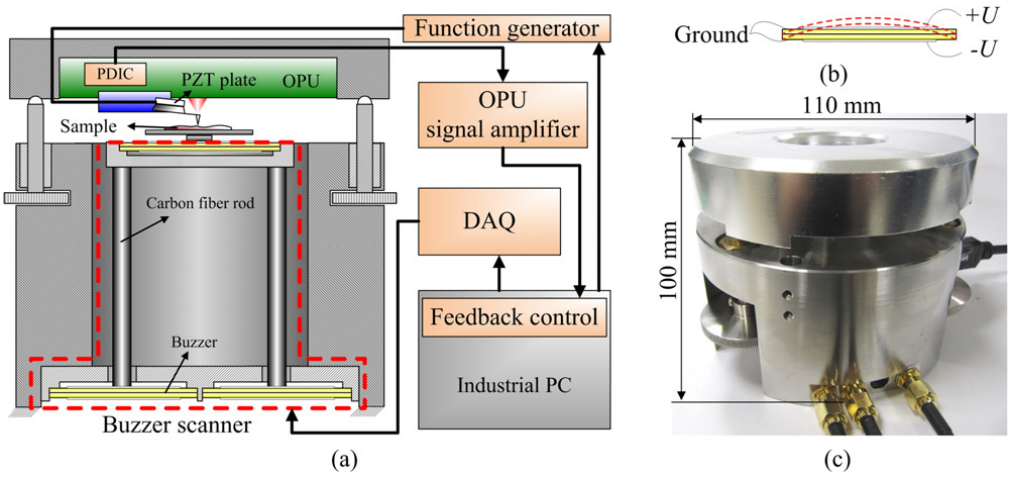

Figure 3. (a) Experimental setup of an OPU-AFM system using the buzzer-scanner. (b) Schematic configuration of a double-layer actuator based on a stack of two disk buzzers. (c) Photo and dimensions of the AFM mechanical part.

where l is the length of the rod, and l_m is the height of the sample holder. According to this equation, the lateral scan range can be increased if longer rods are used. Another way to increase the lateral scan range is to reduce the separation of the two disk buzzers, r, but this method is limited by the diameter of the disk buzzers. Using larger disk buzzers may result in a larger deformation Δl_z, but the separation of the two disk buzzers, r, also needs to be increased, which almost neutralizes the benefit of large disk buzzers in the lateral scan range. A larger buzzer does provide larger movement in the Z axis, but the working bandwidth would be reduced.

The buzzer-scanner was built in a modular form and can be easily fabricated and assembled. The characteristics for commercial disk buzzers of the same model are nearly identical, and no physical machining or modification on any buzzer is involved in this design. Auxiliary assembly jigs were developed and applied to accomplish the precision assembly. Thus the scanning quality and orthogonality of each buzzer-scanner can be easily maintained. Another advantage is that the scanner can be driven directly with a low-voltage and low-current source, such as analog outputs of a data acquisition (DAQ) card. With ± 10 V driving signals from a DAQ card, the buzzer-scanner can provide movement of 5–100 μm in the XY directions, and of 0.5–10 μm in the Z direction, depending on the dimensions of the actuation structure and the type of disk buzzer. This actuation range is sufficient for most AFM applications. The stiffness of the buzzer-scanner can be further increased using two buzzers for each actuation element, as illustrated in figure 3(b).

We constructed an OPU-AFM that uses a buzzer-scanner, and evaluated its scanning characteristics. An experimental setup of the OPU-AFM system is shown in figure 3(a). The buzzer-scanner is fixed on the lower part of the AFM. The buzzer-scanner has the design shown in figure 2(a) with carbon-fiber rods of 3 mm in diameter. The upper plate has four holes (3 mm in diameter with +0.01 mm tolerance) for fixing and guiding the carbon-fiber rods. We used the analog outputs of a DAQ (USB-6351, National Instrument Co.,

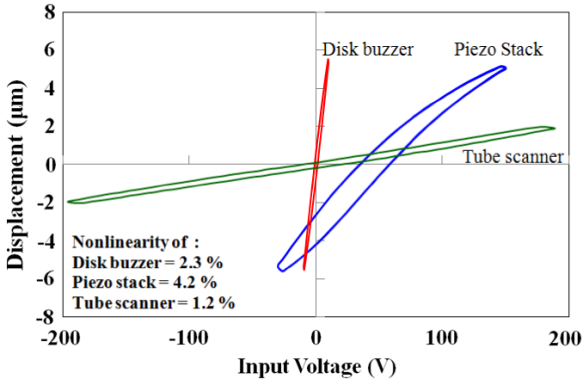

Figure 4. Reciprocating actuation displacements versus the applied voltages measured on a disk buzzer, a piezo-stack, and a tube scanner in the Z axis. The triangular driving signal for the disk buzzer, the piezo-stack, and the tube scanner varies from −10 V to +10 V, −30 V to +150 V, and −200 V to +200 V, respectively, at 0.5 Hz.

maximum current of 5 mA) to drive the buzzer-scanner directly. This OPU-AFM is small and compact, as shown in figure 3(c).

3. Experimental verification and comparisons

3.1. Actuation displacement and nonlinearity evaluation

Figure 4 shows the reciprocating actuation displacements of a 27-mm-diameter disk buzzer (AE-2720E-N, Advanced Acoustic Technology Co.), a 7-mm-long piezo-stack (PSt 150/5 × 5/7, Piezomechanik GmbH) and a tube scanner (17 μm × 17 μm × 3.7 μm in the X, Y, and Z directions, 9910EVLR for Multimode NanoScope IIIa, Digital Instrument) in the Z axis measured with a laser interferometer (SP-S series, SIOS Meßtechnik GmbH). The allowed driving voltage for the disk buzzer, the piezo-stack, and the tube scanner along their polarization direction is −30 to +30 V, −30 to +150 V, and −200 V to +200 V, respectively. For a driving voltage of 1 V, the disk buzzer, the piezo-stack, and the tube scanner in the Z axis can create displacements of 470, 61, and 9.3 nm, respectively. Clearly, the disk buzzer produced a significantly larger displacement than the other two for the same driving amplitude. Thus we drove the disk buzzer with a triangular wave from −10 to +10 V, which can be produced easily from analog outputs of typical data acquisition cards, for the measurement shown in figure 4.

From the hysteresis curves shown in figure 4, one can see a significantly larger nonlinearity for the piezo-stack. The disk buzzer and the tube scanner exhibit an improved linearity. The disk buzzer has the smallest hysteresis in the reciprocating experiments. These measurements were repeated for numerous cycles and the hysteresis curves remained the same for each cycle. We also calculated nonlinearity in these three reciprocating actuation displacements. The definition of nonlinearity can be estimated

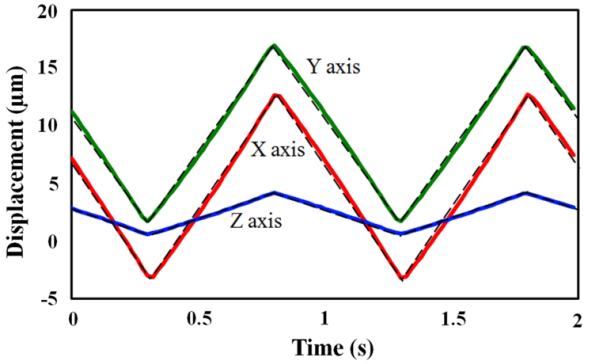

Figure 5. Nonlinearity test of a buzzer-scanner. Nonlinearities on X, Y, and Z-axes are 2.11%, 2.73%, 2.19%, respectively.

by

$$\text{Nonlinearity}\,(\%) = \left(\frac{e_{\max}}{D_{\mathrm{R}}}\right) \times 100, \tag{2}$$

where D_{R} is the full range of measured displacement, and $e_{\max}$ is the maximum error when compared with the ideal linear displacement. The disk buzzer had a full vertical displacement range of 9.5 μm with a nonlinearity of 2.3%, but the piezo-stack had a larger nonlinearity of 4.2% in the same displacement range. The tube scanner has a lower nonlinearity of 1.2% in the Z axis for the displacement range of 3.7 μm. The capacitance of the disk buzzer was only 45 nF, which is much smaller than that of a piezo-stack (800 nF) and slightly larger than that of the tube scanner (25 nF). A DAQ card can thus easily drive a disk buzzer at a frequency of several kilohertz without additional voltage or current amplifiers. In comparison, actuation of a piezo-stack or a tube scanner requires a high-voltage amplifier. Additionally, a high driving current is needed for a piezo-stack. Thus the cost of the electronics for driving a piezo-stack or a tube scanner is significantly higher than that for driving a disk buzzer.

We also measured nonlinearity of the three-axis displacements of the buzzer-scanner. Figure 5 shows the movements in the X, Y and Z directions in response to a triangular driving signal from −10 to +10 V. The displacements were measured separately with the laser interferometer. In this buzzer-scanner, the double-layer actuator shown in figure 3(b) was used for the Z actuation, to increase the stiffness, and single disk buzzer elements were used for the lateral scanning. The displacement ranges were 15 μm, 15 μm, and 3.5 μm in the X, Y, and Z directions with nonlinearity of 2.11%, 2.73%, and 2.19%, respectively. The low and similar nonlinearity in the three axes indicates a favorable quality of the piezoelectric buzzer-scanner. When Z actuation of the buzzer-scanner was driven by a 16-bit DAQ card with analog outputs of ±10 V, the uncertainty of one bit was estimated to be 0.305 mV which corresponds to a theoretical noise level of 0.05 nm. According to our experiment results, the noise level of the Z axis is about 0.06 nm, which is capable of resolving atomic scale features.

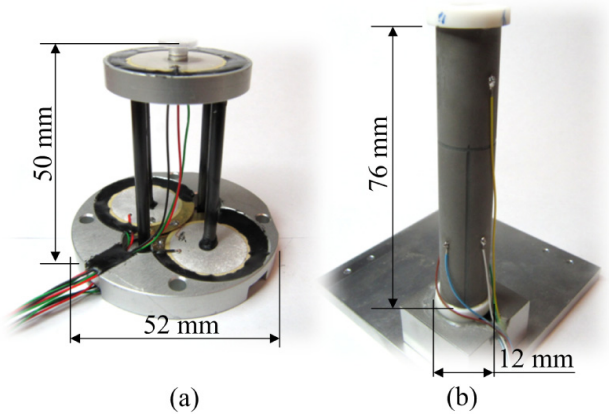

Figure 6. Dimensional comparison between (a) the buzzer-scanner and (b) a tube scanner.

3.2. Comparison of the resonance frequencies between the buzzer-scanner and the tube scanner

The mechanical stiffness of the scanner influences its resonance frequency, which also determines its dynamic scanning performance. Figures 6(a) and (b) show the dimensional comparison between the buzzer-scanner and the tube scanner (EBL #1, EBL Products, Inc.). The tube scanner had full actuation strokes of 17 μm, 17 μm, and 4 μm in the X, Y, and Z directions, respectively, in response to a driving signal from -200 to $+200$ V for each axis. An astigmatic detection system (ADS) measured the resonance frequencies in the X, Y, and Z directions for the two scanners [17]. The scanners of each axis are driven by a sinusoidal wave of various frequencies. Figure 7 shows the measured resonance frequencies in the X, Y, and Z axes. The frequencies of the first resonance mode were similar in these two scanners in the X and Y axes. However, the resonance frequency difference of the buzzer-scanner between the X and Y axes was only 11 Hz (approximately 3%), and that of the tube scanner was 58 Hz (approximately 17%). This indicates a more favorable symmetry for the buzzer-scanner than that of the tube scanner. This may be attributed to the uniform quality of the commercial disk buzzers, with all buzzers having almost identical characteristics. The relatively large differences among the tube scanners may be induced by inhomogeneous structure and/or piezoelectric material deviation.

As shown in figure 7, the buzzer-scanner has a lower resonance frequency of 4.12 kHz and a significantly lower quality factor of 8.68 in the Z axis compared to those of the tube scanner (9.93 kHz and 36.15, respectively). In fact, the lower quality factor would allow a lower overshoot and a shorter settling time in response to a fast driving voltage change. To improve the working bandwidth, one can also stack two disk buzzers or choose disk buzzers of higher resonance frequencies. However, if the disk buzzers with a higher resonance frequency were to be applied, the displacement range would be sacrificed, and the resonance frequency and displacement range of the buzzer-scanner would be compromised.

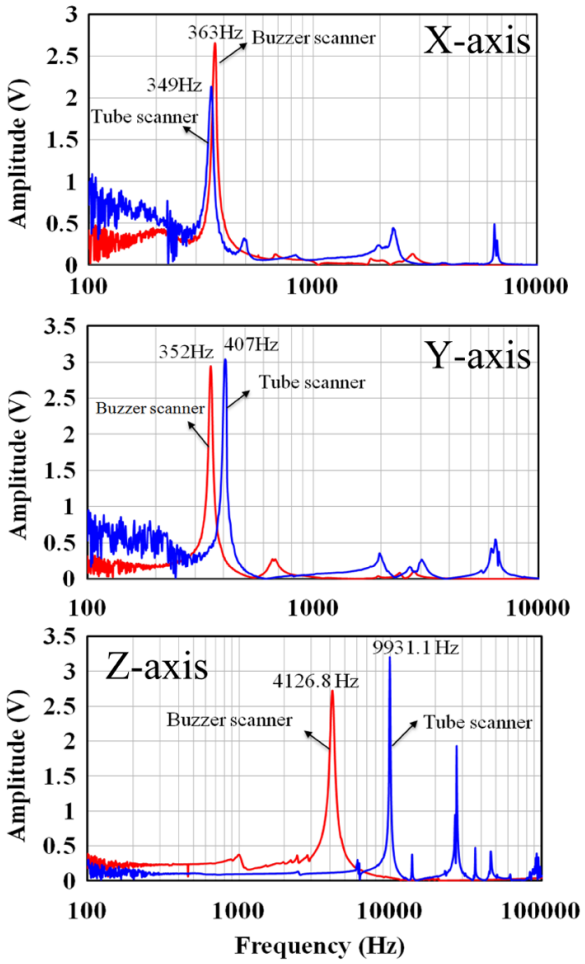

Figure 7. Measurements of resonance frequencies of the buzzer-scanner and the tube scanner in the X, Y and Z axes.

3.3. Orthogonality evaluation for X–Y scanning

To evaluate the orthogonality of the buzzer-scanner, we used the OPU-AFM, as illustrated in figure 3(a), to image standard-AFM calibration samples. Additionally, we compared the performance with another AFM (Multimode NanoScope IIIa from Digital Instruments) that uses the tube scanner shown in figure 6(b). Both scanners are driven by symmetrical triangular wave signals for X and Y sample scanning, without nonlinear or hysteresis compensation. The only image processing required was to remove the angular tilt of the sample surfaces. Figure 8(a) shows a topographic image of a sample (Waffle Grating Replica, Ted Pella) measured with the OPU-AFM equipped with the buzzer-scanner. The sample contained a criss-cross pattern with two sets of straight lines perpendicular to each other. As demonstrated in the AFM image, the two sets of lines intersected each other at an angle of nearly 90°. One was measured to be 90.5°. This indicates that the displacements of the buzzer-scanner in the X and Y axes were almost orthogonal to each other. A slight distortion of the pattern can be seen at various points along the edge of the image.

Figures 8(b) and (c) show the topographic image of an additional calibration sample containing a test grating

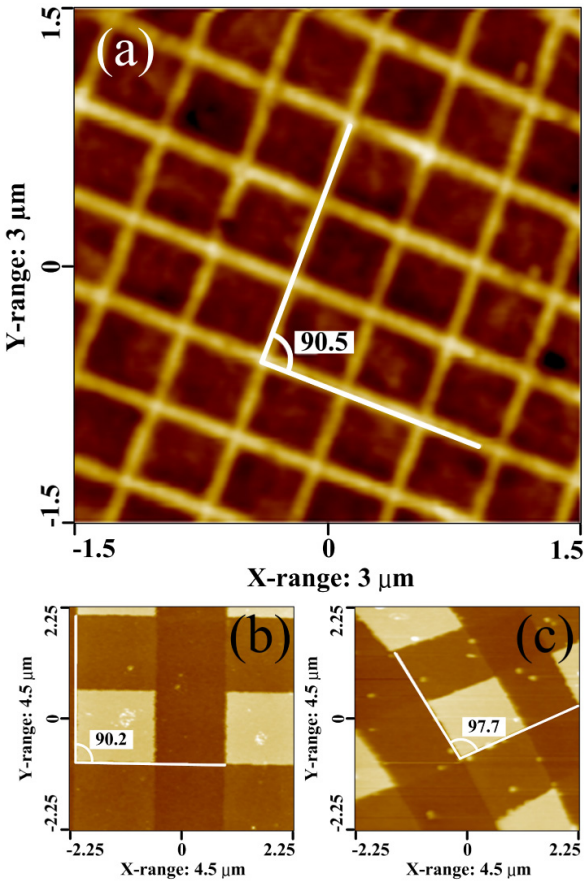

Figure 8. Orthogonality in the *X*–*Y* scanning motions for the buzzer-scanner and the tube scanner with a scanning rate of 1 Hz. (a) Topographic image of a waffle-grating replica measured with an AFM using the buzzer-scanner with the tapping mode. The scan size is 3 μm × 3 μm. (b) Topographic image of a calibration sample measured with an AFM using the buzzer-scanner with the tapping mode. The scan size is 4.5 μm × 4.5 μm. (c) Topographic image obtained with a commercial AFM using a tube scanner. The scan size is 4.5 μm × 4.5 μm.

(TGQ1, NT-MDT) taken with the buzzer-scanner and a tube scanner used in a commercial AFM (9910EVLR for Multimode NanoScope IIIa, Digital Instrument), respectively. We measured the angle at the corner of a square pattern. The ideal angle should measure 90°; we obtained a measurement of 90.2° for the buzzer-scanner, and 97.7° for the tube scanner. This demonstrates that images taken with the buzzer-scanner were less distorted. The error in orthogonality for the tube scanner may be caused by the asymmetrical electrodes of the piezo-tube, or by the inhomogeneity of the piezoelectric material. The favorable orthogonality of the buzzer-scanner may be ascribed to the uniform quality of the commercial disk buzzers and the symmetrical design of the scanner. The disadvantages of the buzzer-scanner are that the actuation force is not as large as the piezo-stack and the resonance frequency of *Z* direction is lower than that of the piezo-tube scanner, and thus the weight of the sample is limited.

3.4. Scanning speed evaluation

The low capacitance of the disk buzzers, or a low-current source from a typical DAQ card, can drive the buzzer-scanner up to 2.25 kHz in the *Z* axis. The *X* and *Y* axis scanning speed is limited by the mechanical resonance, yet the buzzer-scanner can still be driven at a relatively high scan-speed. A highly ordered pyrolytic graphite (HOPG) surface, which has relatively flat areas that are suitable for high scanning speeds, was used as a test sample. When the surface was imaged with a tip velocity $V_{\text{tip}} = 28\ \mu\text{m s}^{-1}$, the topographic image was still clear, as shown in figure 9(a). In figure 9(b), when $V_{\text{tip}} = 40\ \mu\text{m s}^{-1}$, the surface appears similar to that shown in figure 9(a), but the edges are not as sharp. Weak boundary ripples (vertical lines) are visible close to the left side of the topography image, as shown in figure 9(c). These ripples have the height range from 0.1 to 0.2 nm with an approximate time period of 3 ms, which corresponds to the resonance frequency of 363 Hz along the *X* axis. Along the fast scanning *X* axis, the reciprocating motion near the turning boundary induces residual vibration.

3.5. Resolution evaluation

Figure 10(a) shows that single atomic layers on the HOPG surface can be clearly resolved by the OPU-AFM using the buzzer-scanner. The resolution in the *Z* axis is below 1 Å. The scanning range and the scan rate are 1.5 × 1.5 μm and 0.8 Hz, respectively. Figure 10(b) shows a topographic image of double-wall carbon nanotubes on a HOPG surface measured in air with the OPU-AFM. The carbon nanotubes can be observed. The height of the carbon nanotubes measured in figure 10(b) is about 1.95 nm. The full width at half maximum (FWHM) of the measured nanotubes is about 58.8 nm. We note that the lateral resolution of the image might be limited by the tip shape rather than by the positioning resolution of the scanner. In addition, carbon nanotubes tend to aggregate into bundles due to van der Waals interactions. Thus the width of the carbon nanotubes is significantly larger than that of individual carbon nanotubes. Nevertheless, the images demonstrate that the measurement stability and the spatial resolution in the vertical direction are comparable with commercial AFMs, most of which use a beam-deflection detection module and a tube scanner.

4. Conclusions

In this study, we have presented a novel design for a buzzer-scanner. In addition, we constructed an economic, high-performance streamlined atomic force microscope, using the buzzer-scanner to move the sample relative to the probe, and using a CD/DVD OPU to detect the mechanical resonance of a microfabricated cantilever. The scanner was composed of a quad-rod actuation structure and several piezoelectric disk buzzers. Commercially available disk buzzers are of relatively economic benefit, uniform quality, high stability, and have a favorable orthogonality. The buzzer-scanner can be actuated with low driving voltages from typical DAQ cards to achieve significant displacement ranges and the displacements exhibit low nonlinearity compared with the piezo-stack and the tube scanner. In addition, the buzzer-scanner is mechanically and electrically more robust than the piezo-scanner. The

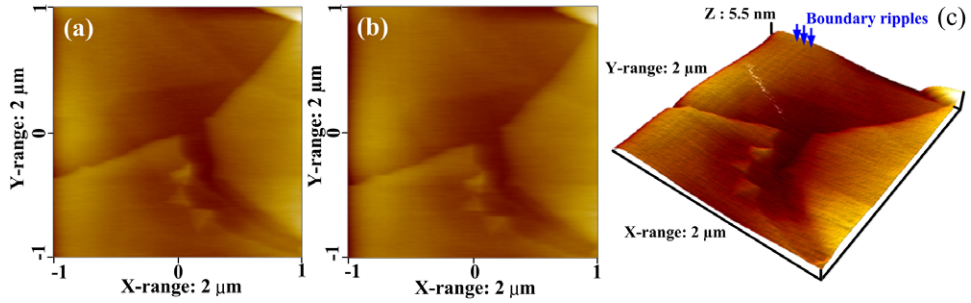

Figure 9. Scanning speed evaluation on HOPG surface. 2 μm × 2 μm topographic images are taken by OPU-AFM at tip velocities of (a) 28 μm s^{-1} and (b) 40 μm s^{-1}. The fast scan direction is from left to right and the slow scan direction is from top to bottom. (c) 3D image of (b). The boundary ripples are indicated with blue arrows.

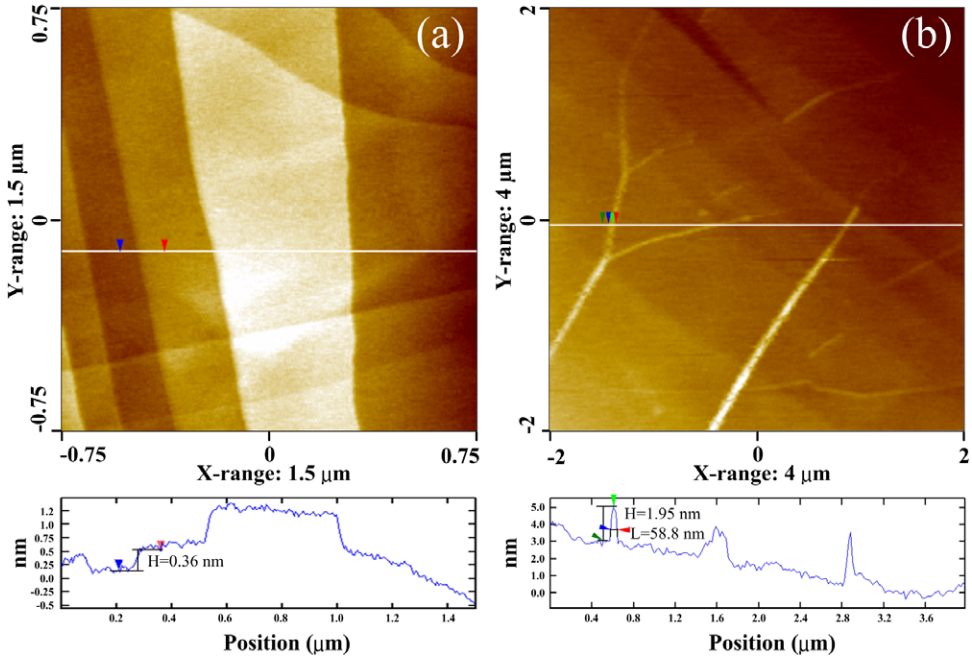

Figure 10. Topographic images taken by the OPU-AFM with the buzzer-scanner. (a) HOPG surface. The scan size is 1.5 μm × 1.5 μm. (b) Double-wall carbon nanotubes on HOPG surface. The scan size is 4 μm × 4 μm.

displacement range of the buzzer-scanner could be further improved by applying a higher driving voltage (maximum 30 V_{p-p}) and the stiffness could be enhanced by using shorter carbon-fiber rods. Commercial disk buzzers cost less than piezoelectric tube scanners and other scanners based on piezo-stacks. Additionally, no current or voltage amplifiers are needed. Therefore, the cost to build an AFM can be reduced significantly. The cost can be further reduced by using a CD/DVD OPU as the detection module of the cantilever movement. This new OPU-AFM can resolve single atomic steps on the HOPG surface with a sub-angstrom resolution, and the scanning speed can reach 40 μm s^{-1}.

To conclude, the OPU-AFM using the buzzer-scanner has a performance compatible with most current commercial AFMs. It does not require costly materials, the structure is small and simple, and no complicated machining process is required. This OPU-AFM design may provide a simple and economic solution for the high-quality nanometer-scale imaging of numerous materials. The design contributes to the goal of making AFM affordable for every lab [3], which may stimulate creativity and discovery in applications and research, as well as in education and training in nanoscience and nanotechnology.

Acknowledgments

The authors would like to thank the machine shop of the Institute of Physics, Academia Sinica for machining the mechanical parts. We also thank Topray Technologies Co. Ltd for providing the optical pickup units. This study was supported by the National Science Council (NSC98-2120-M-001-007-CC2) and Academia Sinica.

References

[1] Wiesendanger R 1994 *Scanning Probe Microscopy and Spectroscopy: Methods and Applications* (Cambridge: Cambridge University Press)

[2] Binnig G, Quate C F and Gerber C 1986 Atomic force microscope *Phys. Rev. Lett.* **56** 930–3
[3] West P 2004 SPM for everyone *Mater. Today* **7** 64
[4] Hwu E T, Huang K Y, Hung S K and Hwang I S 2006 Measurement of cantilever displacement using a compact disk/digital versatile disk pickup head *Japan. J. Appl. Phys.* 1 **45** 2368–71
[5] Hwu E T, Hung S K, Yang C W, Hwang I S and Huang K Y 2007 Simultaneous detection of translational and angular displacements of micromachined elements *Appl. Phys. Lett.* **91** 221908
[6] Hwu E T, Hung S K, Yang C W, Huang K Y and Hwang I S 2008 Real-time detection of linear and angular displacements with a modified DVD optical head *Nanotechnology* **19** 115501
[7] Hwu E T, Illers H, Wang W M, Hwang I S, Jusko L and Danzebrink H U 2012 Anti-drift and auto-alignment mechanism for an astigmatic atomic force microscope system based on a digital versatile disk optical head *Rev. Sci. Instrum.* **83** 013703
[8] Hwu E T, Illers H, Jusko L and Danzebrink H U 2009 A hybrid scanning probe microscope (SPM) module based on a DVD optical head *Meas. Sci. Technol.* **20** 084005
[9] Binnig G and Smith D P E 1986 Single-tube 3-dimensional scanner for scanning tunneling microscopy *Rev. Sci. Instrum.* **57** 1688–9
[10] Yamada H, Fujii T and Nakayama K 1989 Linewidth measurement by a new scanning tunneling microscope *Japan. J. Appl. Phys.* 1 **28** 2402–4
[11] Lee D Y, Kim D M and Gweon D G 2006 Design and evaluation of two dimensional metrological atomic force microscope using a planar nanoscanner *Japan. J. Appl. Phys.* 1 **45** 2124–7
[12] Croft D, Shed G and Devasia S 2001 Creep, hysteresis, and vibration compensation for piezoactuators: atomic force microscopy application *Trans. ASME, J. Dyn. Syst. Meas. Control* **123** 35–43
[13] Fett T and Thun G 1998 Determination of room-temperature tensile creep of PZT *J. Mater. Sci. Lett.* **17** 1929–31
[14] Ge P and Jouaneh M 1996 Tracking control of a piezoceramic actuator *IEEE Trans. Control Syst. Technol.* **4** 209–16
[15] Yun S, Ham Y B, Kim C Y and Park J H 2006 Hysteresis nonlinearity compensator for piezoelectric actuator *J. Electroceram.* **17** 573–6
[16] Alexander J D, Tortonese M and Nguyen T 1999 Atomic force microscope with integrated optics for attachment to optical microscope *US Patent Specification* 5,952,657
[17] Hwu E-T, Liao H-S, Bosco F G, Chen C-H, Keller S S, Boisen A and Huang K-Y 2012 An astigmatic detection system for polymeric cantilever-based sensors *J. Sensors* **2012** 7